

Photochemical properties of Spinach and its use in selective imaging (Supporting information)

Pengcheng Wang,^[a,b] Jérôme Querard,^[a] Sylvie Maurin,^[a] Sarang S. Nath,^[a]
Thomas Le Saux,^{[a,c],*} Arnaud Gautier,^{[a],*} Ludovic Jullien^{[a,c],*}

^[a]*Ecole Normale Supérieure, Département de Chimie,
UMR CNRS-ENS-UPMC Paris 06 8640 Pasteur,
24, rue Lhomond, 75231 Paris Cedex 05, France.
E-mail: Thomas.Lesaux@ens.fr; Arnaud.Gautier@ens.fr; Ludovic.Jullien@ens.fr*

^[b]*Institut Curie, Centre de Recherche, UMR 176 CNRS-Institut Curie,
26 rue d'Ulm, 75248 Paris, France.*

^[c]*UPMC Univ Paris 06,
4 Place Jussieu, 75232 Paris Cedex 05, France.*

1 Theoretical model for the *cis*-DFHBI-Spinach RNA association experiments

In the absence of any photoisomerization, the temporal evolution of the solution composition resulting from mixing solutions of *cis*-DFHBI and Spinach RNA is governed by Eq.(1):



The kinetic law associated with reaction (1) in a homogeneous solution follows:

$$\frac{d\mathbf{1B}(t)}{dt} = k_{+,1} \mathbf{1F}(t)R(t) - k_{-,1} \mathbf{1B}(t). \quad (2)$$

Being in excess with respect to R in the series of stopped-flow experiments, the concentration of fluorophore $\mathbf{1F}$ was assumed constant in both mixed solutions such that $\mathbf{1F}(t) = \mathbf{1F}_{tot}$. Upon considering the total concentration in \mathbf{R} , $R_{tot} = R(t) + \mathbf{1B}(t)$, Eq. (2) yields:

$$\mathbf{1B}(t) = \frac{k_{+,1}\mathbf{1F}_{tot}}{k_{+,1}\mathbf{1F}_{tot} + k_{-,1}} \left(1 - e^{-t/\tau_{1,\pm}}\right) R_{tot}, \quad (3)$$

with

$$\tau_{1,\pm} = (k_{+,1}\mathbf{1F}_{tot} + k_{-,1})^{-1}. \quad (4)$$

Eq.(3) can be used to derive the temporal dependence of the normalized fluorescence intensity $I_F(t)/I_F(0)$:

$$\frac{I_F(t)}{I_F(0)} = 1 + q_1 k_{+,1} R_{tot} \tau_{1,\pm} \left(1 - e^{-t/\tau_{1,\pm}}\right), \quad (5)$$

where $q_1 = \frac{Q_{\mathbf{1B}}}{Q_{\mathbf{1F}}}$ designates the relative brightness between $\mathbf{1B}$ and $\mathbf{1F}$.

2 Theoretical analyses

In this section, we theoretically analyze the dynamic behavior of the models displayed in Scheme 2 of the Main Text. Sharing in common nodes and exchanging processes, those dynamic models only differ by the number of considered nodes and exchanging processes. Instead of exploring stepwise those models, we first consider the most complete model (shown in Scheme 2d), from which we derive the behavior of the simpler models.

2.1 The generic dynamic model

The generic dynamic model is a four-state mechanism consisting of two *trans*-DFHBI states (bound and unbound) in addition to the previously reported *cis* states of DFHBI. Both *cis*- and *trans*-DFHBI interact with Spinach RNA to yield the corresponding fluorescent bound states, Spinach-*cis*-DFHBI and Spinach-*trans*-DFHBI. The two isomers interconvert by photoisomerization in both the bound and unbound states while only *trans-cis* isomerization may occur by thermally-driven exchange. For simplicity, this section uses the symbols **1F**, **2F**, **1B**, and **2B** to represent *cis*-DFHBI, *trans*-DFHBI, Spinach-*cis*-DFHBI, and Spinach-*trans*-DFHBI respectively. The associated rate constants are presented in Figure S1, where the superscripts *hν* and Δ respectively denote photochemical and thermal contributions.^a

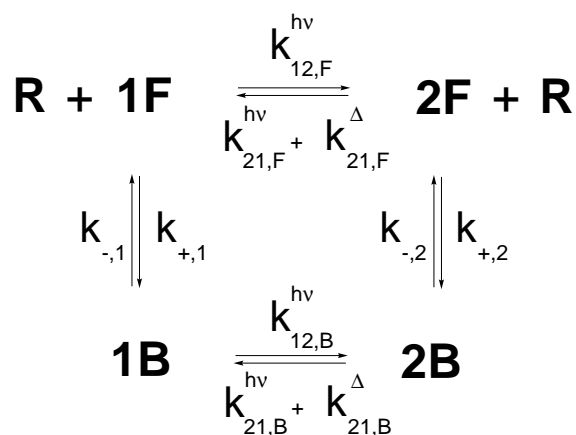


Figure S1: Four-state mechanism accounting for the photochemical and complexation behavior of a photochromic fluorogen in the presence of a receptor.

The theoretical framework closely mirrors that described in a previous work by Emond et al.¹ The concentration profiles within the four state model are governed by the equations:

^a1H-NMR evidence suggests a high purity of the **1F** state prior to illumination, i.e. $k_{12,F}^{\Delta} \ll k_{21,F}^{\Delta}$. Thermal contributions were thus neglected for the forward exchange from **1F** and **2F** to **1B** and **2B** respectively.

$$\frac{d1B}{dt} = -(k_{1B \rightarrow 1F} + k_{1B \rightarrow 2B}) 1B + k_{2B \rightarrow 1B} 2B + k_{1F \rightarrow 1B} R 1F \quad (6)$$

$$\frac{d2B}{dt} = k_{1B \rightarrow 2B} 1B - (k_{2B \rightarrow 2F} + k_{2B \rightarrow 1B}) 2B + k_{2F \rightarrow 2B} R 2F \quad (7)$$

$$\frac{d1F}{dt} = k_{1B \rightarrow 1F} 1B - (k_{1F \rightarrow 1B} R + k_{1F \rightarrow 2F}) 1F + k_{2F \rightarrow 1F} 2F \quad (8)$$

$$\frac{d2F}{dt} = k_{2B \rightarrow 2F} 2B + k_{1F \rightarrow 2F} 1F - (k_{2F \rightarrow 2B} R + k_{2F \rightarrow 1F}) 2F \quad (9)$$

The temporal dependence of concentrations cannot be obtained in the most general case. However, it can be analyzed in asymptotic situations according to the nature of the rate-limiting steps, which are associated to either the photochemical reactions or the complexation reactions. Crossing between both kinetic regimes typically occurs when the relaxation times associated to the photoisomerization and the complexation reactions are equal. Relying on the values subsequently extracted for the Spinach system at the micromolar concentrations used in the present study (*vide infra*), we predicted that photoisomerization would remain rate-limiting up to $2.25 \times 10^{-2} \text{ ein.s}^{-1} \cdot \text{m}^{-2}$,^b a value lying much above our typical light flux. Thus we reduced further theoretical analysis in the following to the regimes where photoisomerization is rate-limiting.

The different dynamic models shown in Scheme 2 correspond to particular values of the rate constants involved in Figure S1. The most general situation corresponding to non-zero values is shown in Scheme 2d. Schemes 2b and 2c are respectively associated to zero values for $k_{12,B}^{h\nu,0}$ and $k_{21,B}^{h\nu,0} + k_{21,B}^{\Delta}$, and for $k_{+,2}$ and $k_{-,2}$, whereas Scheme 2a is associated to zero values for $k_{12,B}^{h\nu,0}$, $k_{21,B}^{h\nu,0} + k_{21,B}^{\Delta}$, $k_{+,2}$, and $k_{-,2}$.

Depending on the values of the rate constants $k_{+,2}$ and $k_{-,2}$, two different reduced schemes result from the reduction of the mechanism displayed in Figure S1 upon considering that photoisomerization is rate-limiting. In the most general situation, $k_{+,2}$ and $k_{-,2}$ adopt non-zero values; then the reduced mechanism involves the exchange between two reduced species (Figure S2a : Two state model). In contrast, when both $k_{+,2}$ and $k_{-,2}$

^bOn the one hand, the relaxation time in a regime where photochemistry is rate-limiting was calculated for increasing light intensities using Eq.(54) and the parameters displayed in Table 1 of the Main Text. On the other hand, the relaxation time in a regime where complexation is rate-limiting was similarly calculated using Eq.(10) which originates from reducing to the corresponding two state model in the case $R_{tot} \ll F_{tot}$:

$$\tau_{\pm}^{F,0} = \frac{1}{k_{\pm}^0 F_{tot} + k_{\pm}^0} \quad (10)$$

with

$$k_{+}^0 = \frac{k_{+,1}^{\Delta} + k_{+,2}^{\Delta} K_F^{h\nu,\Delta,0}}{1 + K_F^{h\nu,\Delta,0}} \quad (11)$$

$$k_{-}^0 = \frac{k_{-,1}^{\Delta} + k_{-,2}^{\Delta} K_B^{h\nu,\Delta,0}}{1 + K_B^{h\nu,\Delta,0}} \quad (12)$$

and

$$K_F^{h\nu,\Delta,0} = \frac{k_{12,F}^{h\nu,0}}{k_{21,F}^{h\nu,0} + k_{21,F}^{\Delta}} \quad (13)$$

$$K_B^{h\nu,\Delta,0} = \frac{k_{12,B}^{h\nu,0}}{k_{21,B}^{h\nu,0} + k_{21,B}^{\Delta}} \quad (14)$$

Then we derived the light intensity for which the two relaxation times were equal.

are equal to zero, the reduced mechanism involves three species and two exchanges (Figure S2b : Three state model).

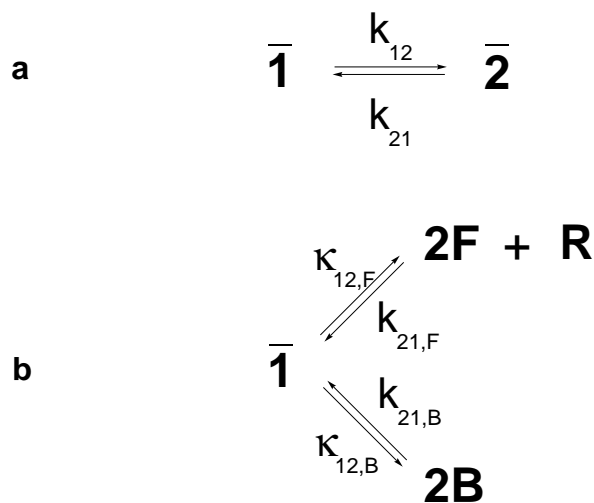


Figure S2: : Models resulting from reduction of the mechanism shown in Figure S1 upon considering that photoisomerization is rate-limiting. **a**: Two state model where $k_{+,2}$ and $k_{-,2}$ adopt non-zero values; **b**: Three state model with $k_{+,2}$ and $k_{-,2}$ equal to zero.

2.2 Analysis of the reduced two state model

In the “low”-illumination regime with non-zero values for $k_{+,2}$ and $k_{-,2}$ (Figure S2a), it is meaningful to introduce the average species $\bar{1}$ and $\bar{2}$ (concentrations $\bar{1} = 1F + 1B$ and $\bar{2} = 2F + 2B$). The “instantaneous” concentrations in **1F**, **1B**, **2F** and **2B** then follow^c,

$$1F = \frac{1}{1 + K_1^\Delta R} \bar{1} \quad (15)$$

$$1B = \frac{K_1^\Delta R}{1 + K_1^\Delta R} \bar{1} \quad (16)$$

$$2F = \frac{1}{1 + K_2^\Delta R} \bar{2} \quad (17)$$

$$2B = \frac{K_2^\Delta R}{1 + K_2^\Delta R} \bar{2} \quad (18)$$

where

$$K_1^\Delta = \frac{k_{+,1}^\Delta}{k_{-,1}^\Delta} \quad (19)$$

$$K_2^\Delta = \frac{k_{+,2}^\Delta}{k_{-,2}^\Delta}. \quad (20)$$

Thus Eqs.(6–9) transform into Eq.(21):

$$\frac{d\bar{1}}{dt} = -\frac{d\bar{2}}{dt} = -k_{12} \bar{1} + k_{21} \bar{2} \quad (21)$$

^cThe association constants, K_1^Δ and K_2^Δ are the inverse of the dissociation constants $K_{d,1}$ and $K_{d,2}$. Furthermore, $k_{+,1}$ and $k_{-,1}$ have been replaced with $k_{+,1}^\Delta$ and $k_{-,1}^\Delta$ to articulate that these rate constants are only affected by temperature rather than light.

with

$$k_{12} = \frac{k_{12,F}^{h\nu} + k_{12,B}^{h\nu} K_1^\Delta R}{1 + K_1^\Delta R} \quad (22)$$

$$k_{21} = \frac{\left(k_{21,F}^{h\nu} + k_{21,F}^\Delta\right) + \left(k_{21,B}^{h\nu} + k_{21,B}^\Delta\right) K_2^\Delta R}{1 + K_2^\Delta R}. \quad (23)$$

In the most general case, Eq.(21) has no analytical solution, because k_{12} and k_{21} are time-dependent as a result of the $R(t)$ term. However, a tractable temporal dependence of the concentrations after a light jump from 0 to I^0 can be obtained in two regimes:

- The total concentration of the receptor (R_{tot}) is much larger than that of the fluorogen (F_{tot}): $R_{tot} \gg F_{tot}$. Then

$$k_{12} = \frac{k_{12,F}^{h\nu} + k_{12,B}^{h\nu} K_1^\Delta R_{tot}}{1 + K_1^\Delta R_{tot}} \quad (24)$$

$$k_{21} = \frac{\left(k_{21,F}^{h\nu} + k_{21,F}^\Delta\right) + \left(k_{21,B}^{h\nu} + k_{21,B}^\Delta\right) K_2^\Delta R_{tot}}{1 + K_2^\Delta R_{tot}}. \quad (25)$$

This case is relevant to analyze the experiments reported in the Main Text when $R_{tot} \gg F_{tot}$.

- The change of light intensity generates a perturbation of the solution composition of small amplitude. As a consequence, Eq.(21) can be solved at first order of light perturbation. This case is relevant to analyze the experiments reported in the Main Text when $F_{tot} \gg R_{tot}$.

2.2.1 Case $R_{tot} \gg F_{tot}$

In such a regime, the apparent rate constant k_{12} and k_{21} can be considered constant and equal to k_{12}^0 and k_{21}^0 given by

$$k_{12}^0 = \frac{k_{12,F}^{h\nu,0} + k_{12,B}^{h\nu,0} K_1^\Delta R_{tot}}{1 + K_1^\Delta R_{tot}} \quad (26)$$

$$k_{21}^0 = \frac{\left(k_{21,F}^{h\nu,0} + k_{21,F}^\Delta\right) + \left(k_{21,B}^{h\nu,0} + k_{21,B}^\Delta\right) K_2^\Delta R_{tot}}{1 + K_2^\Delta R_{tot}}. \quad (27)$$

Since $F_{tot} = \bar{1} + \bar{2}$, Eq.(21) becomes:

$$-\frac{d\left(\bar{2} - \bar{2}^0\right)}{dt} = \left(k_{12}^0 + k_{21}^0\right) \left(\bar{2} - \bar{2}^0\right) \quad (28)$$

without any restriction on the amplitude of light jump. Then Eq.(28) leads to

$$\bar{2} - \bar{2}^0 = \bar{1}^0 - \bar{1} = -\bar{2}^0 \exp\left(-\frac{t}{\tau_{12}^0}\right) \quad (29)$$

where

$$\bar{2}^0 = \frac{K_{12}^0}{1 + K_{12}^0} F_{tot} \quad (30)$$

$$\bar{1}^0 = \frac{1}{1 + K_{12}^0} F_{tot} \quad (31)$$

$$1F^0 = \frac{1}{1 + K_1^\Delta R_{tot}} \bar{1}^0 \quad (32)$$

$$2F^0 = \frac{1}{1 + K_2^\Delta R_{tot}} \bar{2}^0 \quad (33)$$

$$1B^0 = \frac{K_1^\Delta R_{tot}}{1 + K_1^\Delta R_{tot}} \bar{1}^0 \quad (34)$$

$$2B^0 = \frac{K_2^\Delta R_{tot}}{1 + K_2^\Delta R_{tot}} \bar{2}^0 \quad (35)$$

$$R^0 = R_{tot} - \left(\frac{K_1^\Delta R_{tot}}{1 + K_1^\Delta R_{tot}} + \frac{K_2^\Delta R_{tot}}{1 + K_2^\Delta R_{tot}} K_{12}^0 \right) \frac{1}{1 + K_{12}^0} F_{tot} \sim R_{tot} \quad (36)$$

$$\tau_{12}^0 = \frac{1}{k_{12}^0 + k_{21}^0} \quad (37)$$

$$K_{12}^0 = \frac{k_{12}^0}{k_{21}^0} \quad (38)$$

In Eqs.(30–38), $\bar{2}^0$, $\bar{1}^0$, $1F^0$, $1B^0$, $2F^0$, $2B^0$, R^0 , τ_{12}^0 , and K_{12}^0 respectively denote the steady-state values of $\bar{2}$, $\bar{1}$, $1F$, $1B$, $2F$, $2B$, and R , the apparent relaxation time associated to the photochemical reactions, and the apparent photoisomerization constant of the fluorogen **F**, in the presence of light at constant intensity I^0 .

2.2.2 Case of a perturbation of small amplitude

In this regime, there is no restriction on the relative concentrations of **R** and **F**. Thus the apparent rate constant k_{12} and k_{21} cannot be anymore considered constant at the investigated time scale. To be able to perform analytical calculations, we consider that the light jump generates a perturbation of small amplitude. Then we solve Eq.(21) at first order of the light perturbation upon writing:

$$\bar{2} = \bar{2}^0 + \varepsilon \bar{2}^1(t) \quad (39)$$

$$\bar{1} = \bar{1}^0 - \varepsilon \bar{2}^1(t) \quad (40)$$

$$R = R^0 + \varepsilon R^1(t) \quad (41)$$

where $\bar{1}^0$, $\bar{2}^0$, and R^0 denote the steady-state value of the concentrations when light of intensity I^0 is applied on the system.^d Note that it is the same first order term which intervenes in Eqs. (39) and (40) since $\bar{1} + \bar{2} = \bar{1}^0 + \bar{2}^0 = F_{tot}$.

In a first step, the relation existing between $\bar{2}^1(t)$ and $\varepsilon R^1(t)$ is extracted. In relation to Eqs.(15–18), we

^dThe analytical expressions of these concentrations cannot be obtained. Indeed the steady-state concentration R^0 is governed by a polynomial equation, which has no analytical solution. In contrast, those values can be derived numerically.

first derive:

$$\frac{1}{1 + K_i^\Delta R} = \frac{1}{1 + K_i^\Delta R^0} \left(1 - \frac{K_i^\Delta R^1}{1 + K_i^\Delta R^0} \varepsilon \right) \quad (42)$$

$$\frac{K_i^\Delta R}{1 + K_i^\Delta R} = \frac{K_i^\Delta R^0}{1 + K_i^\Delta R^0} \left(1 + \frac{R^1}{R^0 (1 + K_i^\Delta R^0)} \varepsilon \right) \quad (43)$$

with $i = 1$ or 2 . Derivation of Eqs.(42,43) only requires that $K_i^\Delta \varepsilon R^1 \ll 1 + K_i^\Delta R^0$. This condition is fulfilled in the most general case as soon as $\varepsilon R^1 \ll R^0$ where the light jump causes a small change of the concentration in **R**. However, it is also interestingly fulfilled without any restriction on the relative values of R^0 and εR^1 when the **R** concentration is low enough so as to have $K_i^\Delta R_{tot} \ll 1$. Then one has both $K_i^\Delta R^0 \ll 1$ and $K_i^\Delta \varepsilon R^1 \ll 1$. This case is relevant to analyze the experiments described in the Main Text.

Then we use Eqs.(16,18) and the conservation law

$$R_{tot} = R + 1B + 2B \quad (44)$$

to yield

$$R^1 = \gamma \bar{2}^1 \quad (45)$$

with

$$\gamma = \frac{\frac{K_1^\Delta R^0}{1 + K_1^\Delta R^0} - \frac{K_2^\Delta R^0}{1 + K_2^\Delta R^0}}{1 + \frac{K_1^\Delta \bar{1}^0}{(1 + K_1^\Delta R^0)^2} + \frac{K_2^\Delta \bar{2}^0}{(1 + K_2^\Delta R^0)^2}} \quad (46)$$

The temporal dependence of k_{12} and k_{21}

$$k_{12}(t) = \frac{k_{12,F}^{h\nu,0} + k_{12,B}^{h\nu,0} K_1^\Delta R(t)}{1 + K_1^\Delta R(t)} \quad (47)$$

$$k_{21}(t) = \frac{\left(k_{21,F}^{h\nu,0} + k_{21,F}^\Delta \right) + \left(k_{21,B}^{h\nu,0} + k_{21,B}^\Delta \right) K_2^\Delta R(t)}{1 + K_2^\Delta R(t)} \quad (48)$$

is then extracted at first order using Eqs.(41,45). We derived

$$k_{12}(t) = k_{12}^0 + \left(k_{12,B}^{h\nu,0} - k_{12,F}^{h\nu,0} \right) \frac{K_1^\Delta \varepsilon \gamma}{(1 + K_1^\Delta R^0)^2} \bar{2}^1(t) \quad (49)$$

$$k_{21}(t) = k_{21}^0 + \left(k_{21,B}^{h\nu,0} - k_{21,F}^{h\nu,0} \right) \frac{K_2^\Delta \varepsilon \gamma}{(1 + K_2^\Delta R^0)^2} \bar{2}^1(t) \quad (50)$$

with

$$k_{12}^0 = \frac{k_{12,F}^{h\nu,0} + k_{12,B}^{h\nu,0} K_1^\Delta R^0}{1 + K_1^\Delta R^0} \quad (51)$$

$$k_{21}^0 = \frac{\left(k_{21,F}^{h\nu,0} + k_{21,F}^\Delta \right) + \left(k_{21,B}^{h\nu,0} + k_{21,B}^\Delta \right) K_2^\Delta R^0}{1 + K_2^\Delta R^0} \quad (52)$$

Eq.(21) is then solved upon using the expressions (39,40,49,50). We derived

$$\frac{d\bar{2}^1}{dt} + \frac{1}{\tau_{12}^0} \bar{2}^1 = 0 \quad (53)$$

with

$$\tau_{12}^0 = \frac{1}{k_{12}^0 + k_{21}^0 + (\gamma_{21}^0 \bar{2}^0 - \gamma_{12}^0 \bar{1}^0)} \quad (54)$$

where

$$\gamma_{12}^0 = (k_{12,B}^{h\nu,0} - k_{12,F}^{h\nu,0}) \frac{K_1^\Delta \gamma}{(1 + K_1^\Delta R^0)^2} \quad (55)$$

$$\gamma_{21}^0 = (k_{21,B}^{h\nu,0} - k_{21,F}^{h\nu,0}) \frac{K_2^\Delta \gamma}{(1 + K_2^\Delta R^0)^2} \quad (56)$$

Considering that the **2** states are not present at initial time, we then obtain:

$$\varepsilon \bar{2}^1(t) = \bar{2} - \bar{2}^0 = \bar{1}^0 - \bar{1} = -\bar{2}^0 \exp\left(-\frac{t}{\tau_{12}^0}\right) \quad (57)$$

where

$$\bar{2}^0 = \frac{K_{12}^0}{1 + K_{12}^0} F_{tot} \quad (58)$$

$$\bar{1}^0 = \frac{1}{1 + K_{12}^0} F_{tot} \quad (59)$$

$$R^0 = R_{tot} - \left(\frac{K_1^\Delta R^0}{1 + K_1^\Delta R^0} \bar{1}^0 + \frac{K_2^\Delta R^0}{1 + K_2^\Delta R^0} \bar{2}^0 \right) \quad (60)$$

$$K_{12}^0 = \frac{k_{12}^0}{k_{21}^0} \quad (61)$$

Equipped with Eqs.(15–18,39,40,42,43) one has also at first order

$$1F(t) = 1F^0 - \frac{1 + K_1^\Delta R^0 + K_1^\Delta \gamma \bar{1}^0}{(1 + K_1^\Delta R^0)^2} \varepsilon \bar{2}^1(t) \quad (62)$$

$$1B(t) = 1B^0 + \frac{K_1^\Delta \gamma \bar{1}^0 - K_1^\Delta R^0 (1 + K_1^\Delta R^0)}{(1 + K_1^\Delta R^0)^2} \varepsilon \bar{2}^1(t) \quad (63)$$

$$2F(t) = 2F^0 + \frac{1 + K_2^\Delta R^0 - K_2^\Delta \gamma \bar{2}^0}{(1 + K_2^\Delta R^0)^2} \varepsilon \bar{2}^1(t) \quad (64)$$

$$2B(t) = 2B^0 + \frac{K_2^\Delta \gamma \bar{2}^0 + K_2^\Delta R^0 (1 + K_2^\Delta R^0)}{(1 + K_2^\Delta R^0)^2} \varepsilon \bar{2}^1(t) \quad (65)$$

with

$$1F^0 = \frac{1}{1 + K_1^\Delta R^0} \bar{1}^0 \quad (66)$$

$$1B^0 = \frac{K_1^\Delta R^0}{1 + K_1^\Delta R^0} \bar{1}^0 \quad (67)$$

$$2F^0 = \frac{1}{1 + K_2^\Delta R^0} \bar{2}^0 \quad (68)$$

$$2B^0 = \frac{K_2^\Delta R^0}{1 + K_2^\Delta R^0} \bar{2}^0 \quad (69)$$

In Eqs.(58–65), $\bar{2}^0$, $\bar{1}^0$, R^0 , $1F^0$, $1B^0$, $2F^0$, $2B^0$, τ_{12}^0 , K_{12}^0 respectively denote the steady-state value of $\bar{2}$, $\bar{1}$, R , $1F$, $1B$, $2F$, $2B$, the apparent relaxation time associated to the photochemical reactions, and the apparent photoisomerization constant of the fluorogen **F**, in the presence of light at constant intensity I^0 .

2.2.3 Analysis of the fluorescence emission

Fluorescence emission $I_F(t)$ originates from summing the individual contributions of the fluorogen-derived species **1F**, **2F**, **1B**, and **2B**. Denoting Q_i for the molecular brightness, one has

$$I_F(t) = (Q_{1F}1F + Q_{2F}2F + Q_{1B}1B + Q_{2B}2B) I^0 \quad (70)$$

where the expressions of $1F$, $2F$, $1B$, and $2B$ depend on the experimental regimes.

The expressions of $1F$, $2F$, $1B$, and $2B$ can be retrieved from Eqs.(15–18) and (29–38) or (57–69). Then one has:

$$I_F = \left[A^0 + (Q_1 - Q_2) \bar{2}^0 \exp\left(-\frac{t}{\tau_{12}^0}\right) \right] I^0 \quad (71)$$

with

$$A^0 = Q_{1F}1F^0 + Q_{2F}2F^0 + Q_{1B}1B^0 + Q_{2B}2B^0 \quad (72)$$

and

- Case $R_{tot} \gg F_{tot}$:

$$Q_2 = \frac{Q_{2F} + Q_{2B}K_2^\Delta R_{tot}}{1 + K_2^\Delta R_{tot}} \quad (73)$$

$$Q_1 = \frac{Q_{1F} + Q_{1B}K_1^\Delta R_{tot}}{1 + K_1^\Delta R_{tot}} \quad (74)$$

- Case of a perturbation of small amplitude:

$$Q_2 = \frac{1 + K_2^\Delta R^0 - K_2^\Delta \gamma \bar{2}^0}{(1 + K_2^\Delta R^0)^2} Q_{2F} + \frac{K_2^\Delta \gamma \bar{2}^0 + K_2^\Delta R^0 (1 + K_2^\Delta R^0)}{(1 + K_2^\Delta R^0)^2} Q_{2B} \quad (75)$$

$$Q_1 = \frac{1 + K_1^\Delta R^0 + K_1^\Delta \gamma \bar{1}^0}{(1 + K_1^\Delta R^0)^2} Q_{1F} + \frac{K_1^\Delta R^0 (1 + K_1^\Delta R^0) - K_1^\Delta \gamma \bar{1}^0}{(1 + K_1^\Delta R^0)^2} Q_{1B} \quad (76)$$

Moreover assuming that the system contains only $\bar{1}$ before illumination and that the brightnesses of both free states can be neglected in the presence of their corresponding bound states (which is the case in the explored regime of Spinach RNA concentration), the temporal evolution of photoinduced fluorescence-loss given in Eq.(71) yields:

$$I_F(t) = I_F(0) \left[1 + (Q_r - 1) \frac{k_{12}^0}{k_{12}^0 + k_{21}^0} \left(1 - e^{-(k_{12}^0 + k_{21}^0)t} \right) \right] \quad (77)$$

with

$$Q_r = \frac{Q_{2B}}{Q_{1B}} \times \frac{K_{d,1} + R_{tot}}{K_{d,2} + R_{tot}} \quad (78)$$

where $I_F(0)$ is the initial fluorescence intensity at $t = 0$, $I_F(t)$ is the fluorescence intensity at time t , and Q_{2B} and Q_{1B} denote the molecular brightnesses of **2B** and **1B** respectively.

2.2.4 Application to various dynamic models

Photoisomerization of the *cis*-DFHBI fluorogen In relation to the photoisomerization of the *cis*-DFHBI fluorogen in the absence of Spinach RNA which was investigated in an independent experiment, we first derive the temporal dependence of the normalized fluorescence intensity upon applying a light jump from 0 to I^0 . Hence we adapted Eq.(71) to derive

$$I_F(t) = I_F(0) \left[1 + \left(\frac{Q_{2F}}{Q_{1F}} - 1 \right) \frac{k_{12}^0}{k_{12}^0 + k_{21}^0} \left(1 - e^{-(k_{12}^0 + k_{21}^0)t} \right) \right] \quad (79)$$

with

$$k_{12}^0 = k_{12,F}^{h\nu,0} \quad (80)$$

$$k_{21}^0 = k_{21,F}^{h\nu,0} + k_{21,F}^{\Delta} \quad (81)$$

Photoisomerization and complexation of the *cis*-DFHBI fluorogen (Scheme 2a) In the regime considered in the Main Text ($R_{tot} \gg F_{tot}$), Eq.(77,78) adopt different expressions upon assuming that the system contains only $\bar{\mathbf{I}}$ before illumination and that the brightnesses of both free states can be neglected in the presence of the bound state(s) (which is the case in the explored regime of Spinach RNA concentration). In the case of the dynamic model displayed in Scheme 2a, one has

$$I_F(t) = I_F(0) \left[1 - \frac{k_{12}^0}{k_{12}^0 + k_{21}^0} \left(1 - e^{-(k_{12}^0 + k_{21}^0)t} \right) \right] \quad (82)$$

with

$$k_{12}^0 = \frac{K_{d,1}}{K_{d,1} + R_{tot}} k_{12,F}^{h\nu,0} \quad (83)$$

$$k_{21}^0 = k_{21,F}^{h\nu,0} + k_{21,F}^{\Delta} \quad (84)$$

When R_{tot} is much larger than $K_{d,1}$, k_{12}^0 becomes notably vanishing. As a consequence, one expects the loss of fluorescence amplitude to vanish and the rate of fluorescence decay ($k_{12}^0 + k_{21}^0$) to decrease, when the total concentration of \mathbf{R} is increased.

Photoisomerization of *cis*-DFHBI and complexation of both *cis*- and *trans*-DFHBI stereoisomers (Scheme 2b) In the case of the dynamic model displayed in Scheme 2b, Eqs.(77,78) are valid with

$$k_{12}^0 = \frac{K_{d,1}}{K_{d,1} + R_{tot}} k_{12,F}^0 \quad (85)$$

$$k_{21}^0 = \frac{K_{d,2}}{K_{d,2} + R_{tot}} k_{21,F}^0 \quad (86)$$

When R_{tot} is much larger than $K_{d,1}$ and $K_{d,2}$, both k_{12}^0 and k_{21}^0 become notably vanishing. As a consequence, one expects the rate of fluorescence decay ($k_{12}^0 + k_{21}^0$) to vanish when the total concentration of \mathbf{R} is increased.

Photoisomerization of and complexation of both *cis*- and *trans*-DFHBI stereoisomers (Scheme 2d) In the case of the dynamic model displayed in Scheme 2d, Eqs.(77,78) are valid with

$$k_{12}^0 = \frac{k_{12,F}^0 K_{d,1} + k_{12,B}^0 R_{tot}}{K_{d,1} + R_{tot}} \quad (87)$$

$$k_{21}^0 = \frac{k_{21,F}^0 K_{d,2} + k_{21,B}^0 R_{tot}}{K_{d,2} + R_{tot}}. \quad (88)$$

2.3 Analysis of the reduced three state model

In the “low”-illumination regime with zero values for $k_{+,2}$ and $k_{-,2}$ (Figure S2b), one can now introduce only one average species $\bar{\mathbf{I}}$ with concentration $\bar{\mathbf{I}} = 1F + 1B$. The “instantaneous” concentrations in $\mathbf{1F}$ and $\mathbf{1B}$ again follow,

$$1F = \frac{1}{1 + K_1^\Delta R} \bar{\mathbf{I}} \quad (89)$$

$$1B = \frac{K_1^\Delta R}{1 + K_1^\Delta R} \bar{\mathbf{I}} \quad (90)$$

where

$$K_1^\Delta = \frac{k_{+,1}^\Delta}{k_{-,1}^\Delta}. \quad (91)$$

Thus Eqs.(6–9) transform into Eqs.(92–94):

$$\frac{d\bar{\mathbf{I}}}{dt} = -(\kappa_{12,F} + \kappa_{12,B}) \bar{\mathbf{I}} + k_{21,F} 2F + k_{21,B} 2B \quad (92)$$

$$\frac{d2F}{dt} = \kappa_{12,F} \bar{\mathbf{I}} - k_{21,F} 2F \quad (93)$$

$$\frac{d2B}{dt} = \kappa_{12,B} \bar{\mathbf{I}} - k_{21,B} 2B \quad (94)$$

with

$$\kappa_{12,F} = \frac{1}{1 + K_1^\Delta R} k_{12,F}^{h\nu} \quad (95)$$

$$k_{21,F} = k_{21,F}^{h\nu} \quad (96)$$

$$\kappa_{12,B} = \frac{K_1^\Delta R}{1 + K_1^\Delta R} k_{12,B}^{h\nu} \quad (97)$$

$$k_{21,B} = k_{21,B}^{h\nu} + k_{21,B}^\Delta. \quad (98)$$

When $R_{tot} \gg F_{tot}$, the system of linear differential equations (92–94) possesses two non trivial negative eigenvalues λ_+ and λ_- associated to two relaxation times τ_+ and τ_- given in the expression (99)

$$\lambda_{\pm} = -\frac{1}{\tau_{\pm}} = -\frac{1}{2}S \pm \frac{1}{2}\sqrt{S^2 - 4(\kappa_{12,F}k_{21,B} + k_{21,F}k_{21,B} + k_{21,F}\kappa_{12,B})} \quad (99)$$

with

$$S = \kappa_{12,F} + k_{21,F} + \kappa_{12,B} + k_{21,B}. \quad (100)$$

Upon assuming that the contribution of the free states **1F** and **2F** to the overall fluorescence emission can be neglected, the temporal evolution of the fluorescence emission occurring after a jump of light intensity from 0 to I^0 is

$$I_F(t) = \bar{I}^0 \left(a_0 + a_+ e^{\lambda_+ t} + a_- e^{\lambda_- t} \right) I^0 \quad (101)$$

with

$$a_0 = \frac{1}{\lambda_+ \lambda_-} \frac{K_1^\Delta R_{tot}}{1 + K_1^\Delta R_{tot}} k_{21,F} \left[Q_{1B} k_{21,B} + Q_{2B} k_{12,B}^{h\nu} \right] \quad (102)$$

$$a_+ = \frac{1}{\lambda_+ (\lambda_+ - \lambda_-)} \frac{K_1^\Delta R_{tot}}{1 + K_1^\Delta R_{tot}} (k_{21,F} + \lambda_+) \left[Q_{1B} (k_{21,B} + \lambda_+) + Q_{2B} k_{12,B}^{h\nu} \right] \quad (103)$$

$$a_- = \frac{1}{\lambda_- (\lambda_- - \lambda_+)} \frac{K_1^\Delta R_{tot}}{1 + K_1^\Delta R_{tot}} (k_{21,F} + \lambda_-) \left[Q_{1B} (k_{21,B} + \lambda_-) + Q_{2B} k_{12,B}^{h\nu} \right] \quad (104)$$

where $\bar{I}^0 = 1F^0 + 1B^0$ designate the steady-state value of the concentration in *cis*-species.

With this model, one correspondingly expects a bi-exponential decay of the temporal evolution of the fluorescence emission.

3 Theoretical computations

The equations (54), (71), (66), (67), (68) and (69) have been first used to compute the relaxation time τ_{12}^0 and the normalized fluorescence loss $\frac{(Q_1-Q_2)\bar{2}^0}{A^0+(Q_1-Q_2)\bar{2}^0}$ as well as the steady-state concentrations $1F^0$, $1B^0$, $2F^0$, and $2B^0$ at $R_{tot} = 0.1 \mu\text{M}$ and $F_{tot} = 1 \mu\text{M}$ for various values of the light intensity I^0 upon using the Spinach-DFHBI features displayed in Table 1 of the Main Text. The results are displayed in Figure S3.

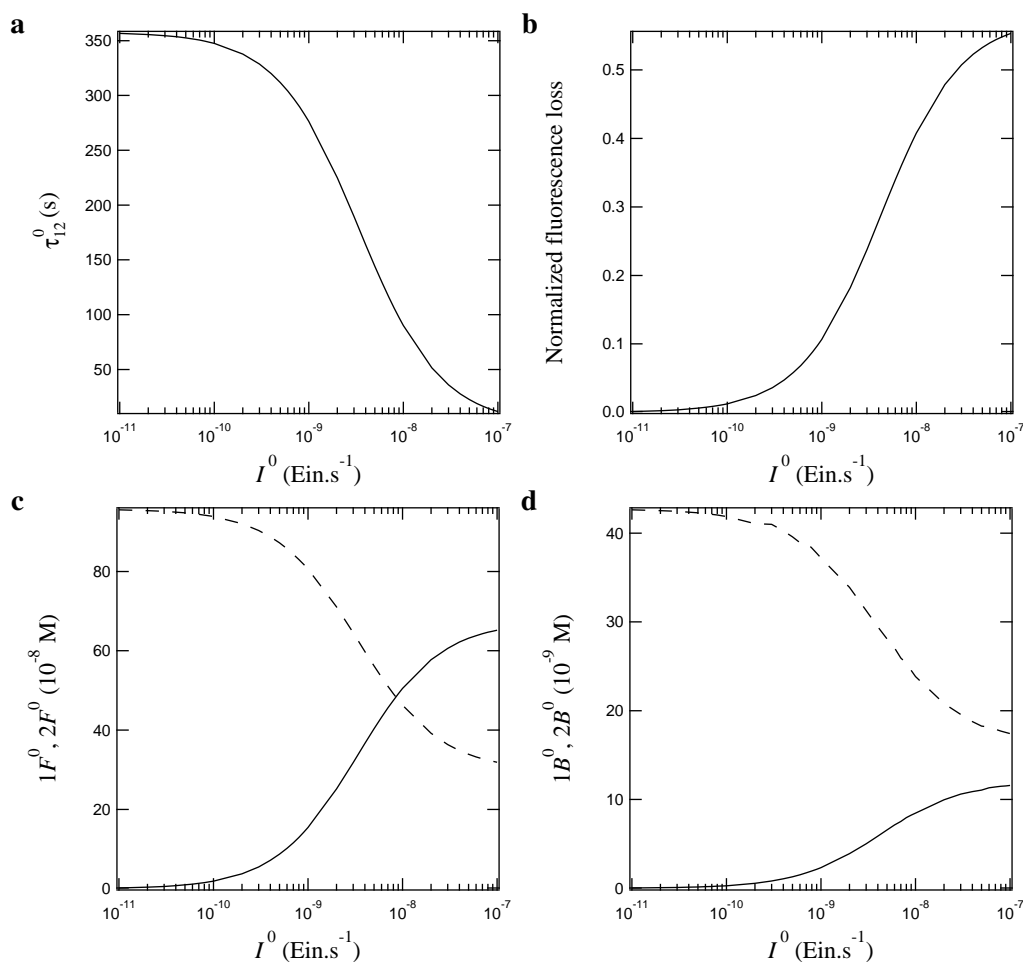


Figure S3: Theoretical computation of the dependence of the relaxation time τ_{12}^0 (**a**), the normalized fluorescence loss $\frac{(Q_1-Q_2)\bar{2}^0}{A^0+(Q_1-Q_2)\bar{2}^0}$ (**b**), the free (**c**; $1F^0$: dotted line; $2F^0$: solid line) and bound (**d**; $1B^0$: dotted line; $2B^0$: solid line) state concentrations on the light intensity I^0 using Eqs. (54), (71), (66), (67), (68) and (69) respectively. $R_{tot} = 0.1 \mu\text{M}$; $F_{tot} = 1 \mu\text{M}$.

The same set of equations have been also used to compute the dependence of the relaxation time τ_{12}^0 , the normalized fluorescence loss $\frac{(Q_1-Q_2)\bar{2}^0}{A^0+(Q_1-Q_2)\bar{2}^0}$, and the steady-state concentrations $1F^0$, $1B^0$, $2F^0$, and $2B^0$ at light intensity $I^0 = 9.0 \times 10^{-9} \text{ ein}\cdot\text{s}^{-1}$ for various values of the total concentrations R_{tot} and F_{tot} upon using the Spinach-DFHBI features displayed in Table 1. The results are displayed in Figures S4a,b and S5a,b.

The significance of the relative total concentrations R_{tot} and F_{tot} on the relaxation time and on the normalized fluorescence loss is weaker than the one of the light intensity I^0 . In fact, it essentially reflects the difference of the photochemical properties between the free and bound DFHBI states (see Table 1).

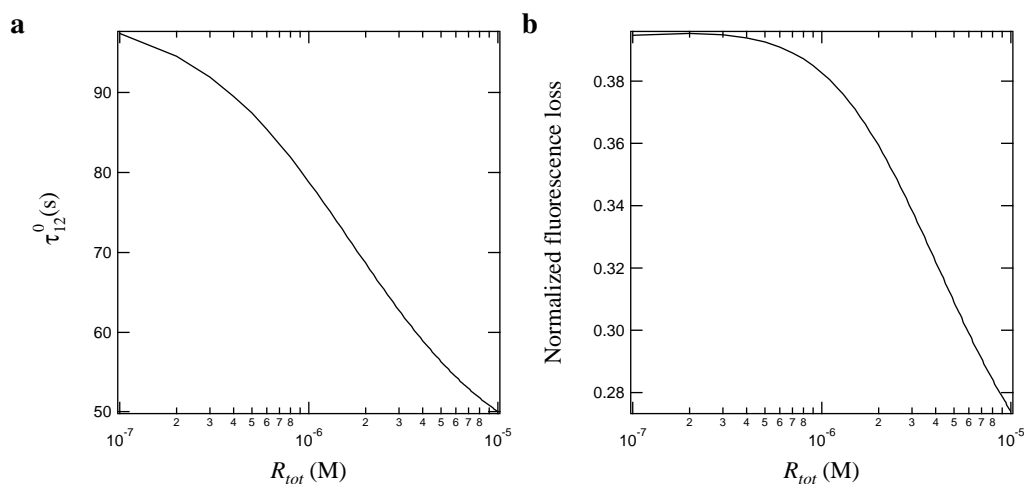


Figure S4: Theoretical computation of the dependence of the relaxation time τ_{12}^0 (a) and the normalized fluorescence loss $\frac{(Q_1-Q_2)\bar{2}^0}{A^0+(Q_1-Q_2)\bar{2}^0}$ (b) on the total RNA concentration at $F_{tot} = 1 \mu\text{M}$ and $I^0 = 9.0 \times 10^{-9} \text{ ein}\cdot\text{s}^{-1}$ using Eqs. (54) and (71) respectively.

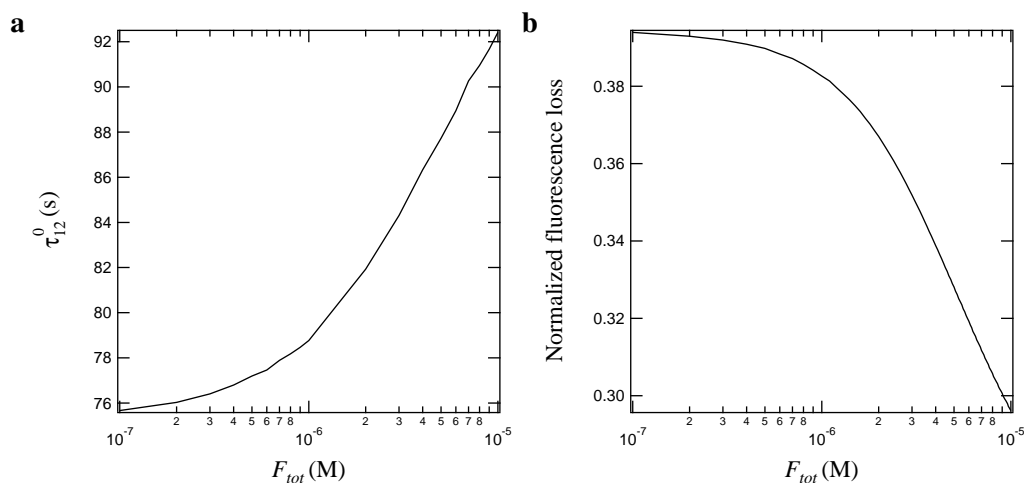


Figure S5: Theoretical computation of the dependence of the relaxation time τ_{12}^0 (a) and the normalized fluorescence loss $\frac{(Q_1-Q_2)\bar{2}^0}{A^0+(Q_1-Q_2)\bar{2}^0}$ (b) on the total DFHBI concentration at $R_{tot} = 1 \mu\text{M}$ and $I^0 = 9.0 \times 10^{-9} \text{ ein}\cdot\text{s}^{-1}$ using Eqs. (54) and (71) respectively.

4 Supplementary Figures

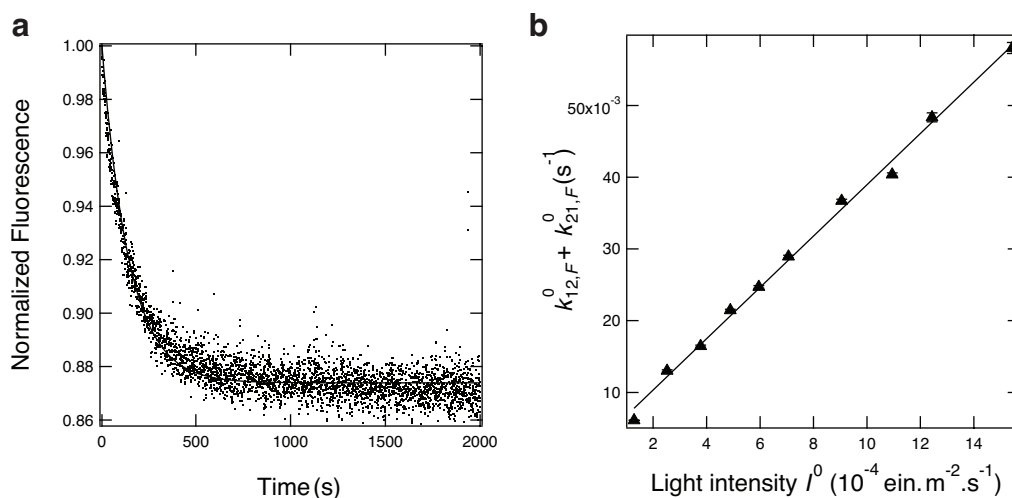


Figure S6: Kinetics of *cis*-DFHBI photoisomerization. **a**: Temporal evolution of the normalized fluorescence emission at 510 nm upon illuminating a 100 μM *cis*-DFHBI solution with 470 nm light (5×10^{-9} ein.s $^{-1}$). Dots: experimental points; solid line: exponential fit with Eq.(3) of the Main Text; **b**: Dependence of the rate constant associated to the fluorescence decay $k_{12,F}^0 + k_{21,F}^0$ on light intensity I^0 . Markers: experimental points; solid line: linear fit. Solvent: pH 7.4 HEPES buffer; T = 293 K.

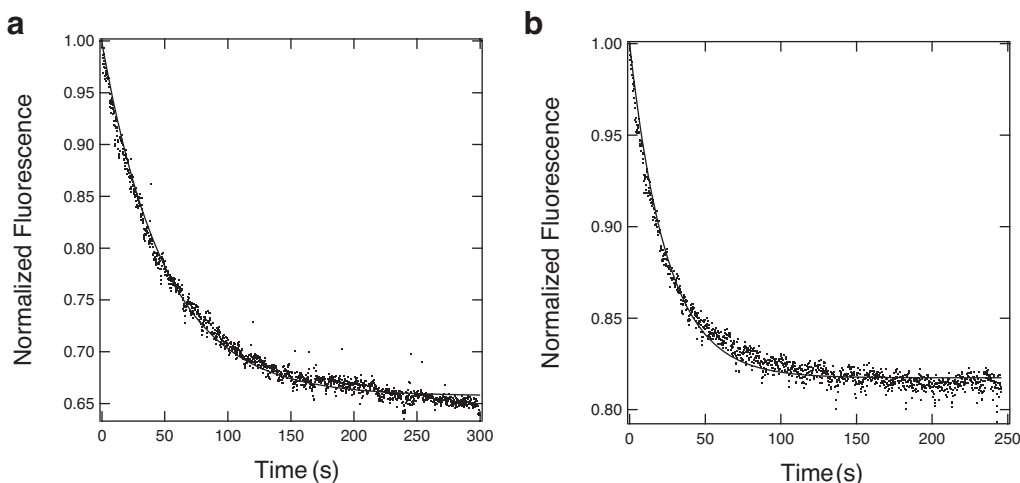


Figure S7: Decay of fluorescence emission at 498 nm of the Spinach system upon illuminating at 470 nm. Temporal evolution of the normalized fluorescence emission at 498 nm upon illuminating a solution containing 0.1 μM *cis*-DFHBI and 1.8 (**a**) or 20 (**b**) μM Spinach RNA with 470 nm light (1.7×10^{-8} ein.s $^{-1}$). Dots: experimental points; solid line: exponential fit with Eq.(4) of the Main Text. Solvent: pH 7.4 HEPES buffer; T = 293 K.

References

- [1] M. Emond, T. Le Saux, S. Maurin, J.-B. Baudin, R. Plasson, L. Jullien, *Chem. Eur. J.* **16**, 8822-8831 (2010).
- [2] J. Dong, F. Abulwerdi, A. Baldrige, J. Kowalik, K. M. Solntsev, L. M. Tolbert, *J. Am. Chem. Soc.*, **130**, 14096-14098 (2008).
- [3] J. S. Paige, K. Y. Wu, S. R. Jaffrey, *Science* **333**, 642-646 (2011).